Volumetric stability of two-step ionization dominated discharges

L. Friedland,[a] J. H. Jacob, and J. A. Mangano
Science Research Laboratory, Incorporated, Somerville, Massachusetts 02143

(Received 17 October 1988; accepted for publication 1 February 1989)

The stability of self-sustained discharges is investigated both analytically and numerically. The dominant ionization mechanism in the discharge is assumed to be two-step ionization while both electron loss mechanisms attachment and recombination are considered. It is shown that the stiff voltage source is marginally stable when the electron loss rate is due solely to electron-molecular ion recombination. In the presence of attachment the stiff voltage source is unstable and the growth rate of the instability is approximately the attachment rate. A stiff current is shown to be more stable and the discharge is stable irrespective of the loss rate. The theory is verified numerically for an atmospheric Co_2 laser discharge.

I. INTRODUCTION

Stability of high-pressure discharges has been a subject of major concerns in the high-power laser community over the last 15 years. Most of the discharge stability research, especially for CO_2 laser discharges, concentrated on thermal instabilities[1] and their effect on the constriction and arcing of the discharge.[2] Vibrational stabilization methods have been proposed to suppress these instabilities.[3]

The thermal instabilities, by their nature, can only develop on the acoustic (millisecond) time scales. However, in many cases[4] the arcing occurs on a much faster (microsecond and submicrosecond) scale. The phenomenon is characteristic of systems where the electron loss by attachment is present and the two-step electron impact ionization is dominant.[4] Such a model successfully explained the experimentally observed temporally rapid instability scales in the KrF laser discharges.[4]

In addition to the KrF discharge case, subacoustic arcing time scales have also been observed in the high-power CO_2 laser experiments. An example of such arcing is in connection with the gas recirculation in the laser, resulting in the buildup of the attaching oxygen component in the laser gas mixture.[5] These observations could be also explained within the two-step ionization model.[4] Although the details of the kinetics in a high-pressure molecular discharge seem to be rather complex, the concept of two-step ionization as the dominant ionization source in the discharge is plausible. The reason is the fact that the electron temperature in these discharges are relatively low (typically 1–2 eV) and very few electrons in the tail of the distribution function can directly ionize the ground state, while the ionization of a variety of available excited and metastable states requires much lower energies and is accessible by the bulk of the electron energy distribution. It is precisely this reason, though speculative in its details, but almost certain in reality, which makes the further development of the multistep ionization discharge theory necessary. This paper considers such a simplified two-step ionization model in describing the operation of the discharge and its stability.

[a] Permanent address: Center for Plasma Physics, Racah Institute of Physics, Hebrew University of Jerusalem, Jerusalem, Israel.

The scope of the paper will be as follows. Section II describes the details of the model and investigates the steady-state operation of the discharge. The volumetric stability of the discharge is discussed in Sec. III for three circuit conditions: a stiff voltage source, stiff current source, and the intermediate finite impedance voltage source. Finally, numerical examples for a CO_2 laser mixture case will be presented in Sec. IV.

II. THE STEADY STATE

Consider a system, shown schematically in Fig. 1 with a dc voltage source V_0. The voltage is distributed between the external resistor R and the plasma, so that

$$V_0 = RI + LE, \tag{1}$$

where I is the discharge current, L is the plasma length, and E is the electric field in the plasma, which is assumed to be uniform at all time. In writing Eq. (1) it is assumed that the cathode fall voltage is negligible compared to LE (a situation typical of *high-pressure* discharges).

Now we shall specify three regimes of operation

(a) Stiff voltage case: Here $R \simeq 0$ and thus the field in the discharge,

$$E = V_0/L = \text{const}, \tag{2}$$

is not affected by a possible temporal variations of discharge characteristics, such as the electron density, temperature, etc.

(b) Stiff current case: In this case $R \to \infty$ and $V_0 \to \infty$, so that the current,

$$I \simeq V_0/R = \text{const}, \tag{3}$$

is time independent and fully described by the external circuit.

(c) Finite external impedance case: In this intermediate case $(0 < R < \infty)$ both the current,

$$I(t) = [V_0 - LE(t)]/R, \tag{4}$$

and the electric field $E(t)$ depend on the details of the time evolution of the discharge.

At this point it will be informative to discuss the kinetics of the self-sustained discharge. The densities of various species in the discharge will be assumed to be spatially uniform,

 0021-8979/89/103790-08$02.40

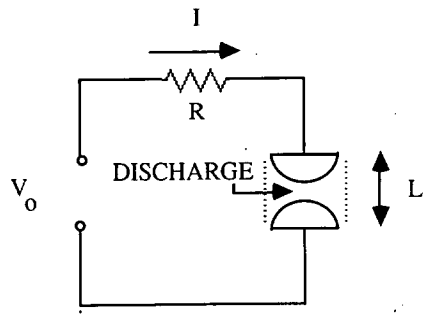

FIG. 1. General circuit model.

and that the discharge is described by the following system of rate equations:

$$\frac{dn_e}{dt} = \nu n_m n_e - \alpha n_e^2 - \beta n_e, \tag{5}$$

$$\frac{dn_m}{dt} = \gamma n_e n_a - \frac{n_m}{\tau}. \tag{6}$$

Here n_e is the electron density, governed by the ionization of an excited or metastable state having a density n_m and by recombination and attachment losses (ν,α, and β are the corresponding rate constants). The density of the excited or metastable state is defined by the balance between the processes of the excitation by electron impact of atoms from the ground state (of density n_a) and the collisional quenching by the neutral gas (with characteristic time constant τ). The time scales τ, (αn_e), and β^{-1} are assumed to be much shorter than the acoustic times and thus the neutral gas temperature and density are constants

Equations (5) and (6) yield the steady state in which all the discharge characteristics are constant and

$$n_m = n_{m0} = \gamma_0 \tau n_{e0} n_a, \tag{7}$$

$$n_e = n_{e0} = \beta_0/(\nu_0 \gamma_0 \tau n_a - \alpha_0). \tag{8}$$

Consider now the question of whether this steady state can be reached for a given set of parameters of the external circuit (V_0, R, and L). The answer to this question depends on the regime of operation.

A. Stiff voltage case

Here $E = E_0$ is given, which defines all the rates in Eq. (8) so that n_{e0} is known. This, in turn, defines the current density $j = e n_{e0} v_{d0}$ in the plasma (v_{d0} being the drift velocity of the electrons). Thus the steady state exists, provided of course [see Eq. (8)] the quantity

$$Q(E_0) \equiv \nu_0 \gamma_0 \tau n_a - \alpha_0 \tag{9}$$

is *positive*. This condition restricts the accessibility of the steady state and needs further discussion. consider the dependence of Q on E_0. Typically, the excitation and ionization rates (γ_0,ν_0) are increasing functions of the electric field, while the attachment rate α_0 normally decreases with E_0. Furthermore, $\lim_{E_0 \to 0} Q \simeq -\alpha_{(E_0 \to 0)} < 0$ and with the increase of E_0, $Q \to \nu_0 \gamma_0 \tau n_a > 0$. Therefore, there exists a *single* value of the electric field $E_0 = E^*$ at which $Q(E^*) = 0$. The steady-state operation of the discharge under the stiff voltage conditions (E_0 is given) is thus only possible when

$$E_0 \simeq V_0/L > E^*. \tag{10}$$

B. Stiff current case

Here the current I_0 is defined by the external circuit. On the other hand, from Eq. (8),

$$I_0 = e v_{d0} n_{e0} S = e v_{d0} \beta_0 S / Q(E_0) \equiv F(E_0), \tag{11}$$

where S is the cross section area of the discharge. Equation (11) now defines the steady-state electric field value E_0. A graphical illustration of the solution of this equation is given in Fig. 2, where the qualitative dependence of function F on E is shown based on our earlier discussion of function $Q(E)$. A possible minimum of F at $E = E_m$ is also shown,. Such a minimum may exist at high values of E_0 at which the ionization and excitation rates grow slower than the drift velocity v_d as the electric field increases. It can be seen in Fig. 2 that the steady state exists for any current I_0, provided it is larger than I_m. It is noteworthy that the operation near E_0^* requires rather high currents.

C. Finite impedance case

In this intermediate case Eq. (11) is replaced by [see Eq. (4) for the current]

$$(V_0 - L E_0)/R = F(E_0). \tag{12}$$

The graphical solution of this equation for E_0 is shown in Fig. 3. We observe that for given values of V_0 there exists a critical impedance R_{cr} such that when $R < R_{cr}$ two steady-state solutions (E_{01} and E_{02}) exist for the electric field, while for $R > R_{cr}$ no steady state exists at all. For $R = R_{cr}$ there is a single steady state. The value of R_{cr} can be found from

$$L = -R_{cr} F'(E_{cr}), \tag{13}$$

where $F' = dF/dE_0$ and E_{cr} is given implicitly by

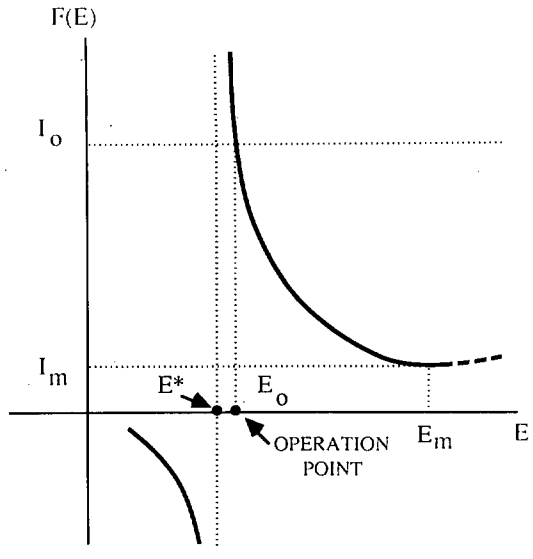

FIG. 2. Graphical solution for the electric field in the discharge under stiff current condition (I_0 is given).

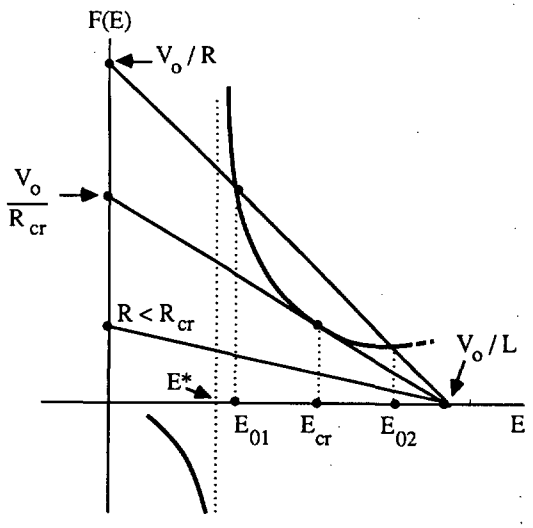

FIG. 3. Graphical solution for the electric field E_0 in the discharge under finite impedance conditions. The straight lines describe the function $(V_0 - LE_0)/R$ for different values of the external impedance R.

$$E_{cr} - (V_0/L) = F(E_{cr})/F'(E_{cr}). \tag{14}$$

This completes the analysis of the possibility of a steady-state solution at various external circuit conditions.

III. VOLUMETRIC STABILITY ANALYSIS

At this stage one can analyze the problem of the stability of the steady-state discharge with respect to a small *uniform* (volumetric) perturbations of the electron and excited state densities. Accordingly, one looks for solutions of Eqs. (5) and (6) in the form

$$n_e(t) = n_{e0} + \delta n_e(t), \quad n_m(t) = n_{m0} + \delta n_m(t), \tag{15}$$

where n_{e0} and n_{m0} are the steady-state solutions described in the previous section and δn_e, δn_m are small perturbations. Again the stiff voltage, stiff current, and finite impedance cases will be considered separately.

A. Stiff voltage case

Since the electric field in the discharge in this case is a constant of time (E_0) all the rates in Eqs. (5) and (6) are also constants of time and, after the linearization, one can write

$$\frac{d(\delta n_e)}{dt} = \nu n_{e0}\delta n_m + (\nu n_{m0} - 2\alpha n_{e0} - \beta)\delta n_e, \tag{16}$$

$$\frac{d(\delta n_m)}{dt} = \gamma n_a \delta n_e - \frac{\delta n_m}{\tau}. \tag{17}$$

Assuming solutions δn_m, $\delta n_e \sim \exp(-i\omega t)$, we then obtain the characteristic equation

$$\omega^2 + i\omega[\alpha n_{e0} + (1/\tau)] + \beta/\tau = 0. \tag{18}$$

The roots of Eq. (18) are

$$\omega_{1,2} = -\frac{i}{2}\left[\left(\alpha n_{e0} + \frac{1}{\tau}\right) \pm \sqrt{\left(\alpha n_{e0} + \frac{1}{\tau}\right)^2 + \frac{4\beta}{\tau}}\right], \tag{19}$$

and, since one of these roots has $\mathrm{Im}\,\omega > 0$, the solution of Eqs. (16) and (17) is generally unstable (except when $\beta = 0$, in which case one of the roots, $\omega_2 = 0$, indicates a marginal stability). It can be also seen that if τ is the shortest characteristic time in the problem, Eq. (19) yields $\omega_2 \simeq i\beta$, i.e., the growth rate is approximately the rate of attachment.

B. Stiff current case

Here, the current $I = ev_d n_e S$ in the discharge remains constant in time, regardless of the variation in the electron density. Therefore,

$$\delta v_d n_{e0} + \delta n_e v_{d0} = 0,$$

and, since

$$\delta v_d = \frac{dv_{d0}}{dE_0}\delta E,$$

the electron density perturbation results in the perturbation of the electric field, given by

$$\delta E = -(v_{d0}\delta n_e / v'_{d_0} n_{e0}), \tag{20}$$

where $v'_{d0} = dv_{d0}/dE_0$. Typically $v'_{d0} > 0$ and thus the variation of the electron density leads to the *opposite* change in the electric field E_0 in the discharge. This, of course, plays a stabilizing role via the appropriate change in the electron production rate. The phenomenon can be demonstrated analytically. Indeed, in the case of interest, perturbed Eqs. (16) and (17) should now be replaced by

$$\frac{d(\delta n_e)}{dt} = \nu_0 n_{e0}\delta n_m + (\nu_0 n_{m0} - 2\alpha_0 n_{e0} - \beta_0)\delta n_e + (\nu'_0 n_{m0} - \alpha'_0 n_{e0}^2 - \beta'_0 n_{e0})\delta E, \tag{21}$$

$$\frac{d(\delta n_m)}{dt} = \gamma_0 n_a \delta n_e - \frac{\delta n_m}{\tau} + \gamma'_0 n_a n_{e0}\delta E, \tag{22}$$

where $\xi' = d\xi/dE_0$ for $\xi = \nu_0, \alpha_0, \beta_0$, and γ_0. The substitution of expression for δE transforms Eqs. (21) and (22) into a system of linear first-order differential equations for δn_e and δn_m. The characteristic equation for this system is

$$\omega^2 + i\omega A + (\beta/\tau) - B = 0, \tag{23}$$

where

$$A = \alpha n_{e0} + \frac{1}{\tau} + \frac{v_{d0}}{v'_{d0}}(n_{m0}\nu'_0 - n_{e0}\alpha'_0 - \beta'_0) \tag{24}$$

and

$$B = \frac{v_{d0}}{v'_{d0}}\left[\alpha_0 n_0 \nu_0 n_{e0}\left(\frac{\nu'_0}{\nu_0} + \frac{\gamma'_0}{\gamma_0}\right) - \frac{\alpha'_0 n_{e0} + \beta'_0}{\tau}\right]. \tag{25}$$

The roots of Eq. (23) are

$$\omega_{1,2} = -(i/2)\left\{A \pm \sqrt{A^2 + 4[(\beta/\tau) - B]}\right\}. \tag{26}$$

Finally, by inspecting Eqs. (5) and (11) one observes that

$$\frac{\beta}{\tau} - B = \frac{Q(E_0)F'(E_0)}{eS\tau v'_{d_0}}, \tag{27}$$

and therefore $\beta/\tau - B < 0$, if $F'(E_0) < 0$. In this case Eq. (26) yields characteristic roots with $\mathrm{Im}\,\omega < 0$ and thus the discharge is *stable* in the decreasing region of function $F(E_0)$ ($E^* < E_0 < E_m$, see Fig. 2).

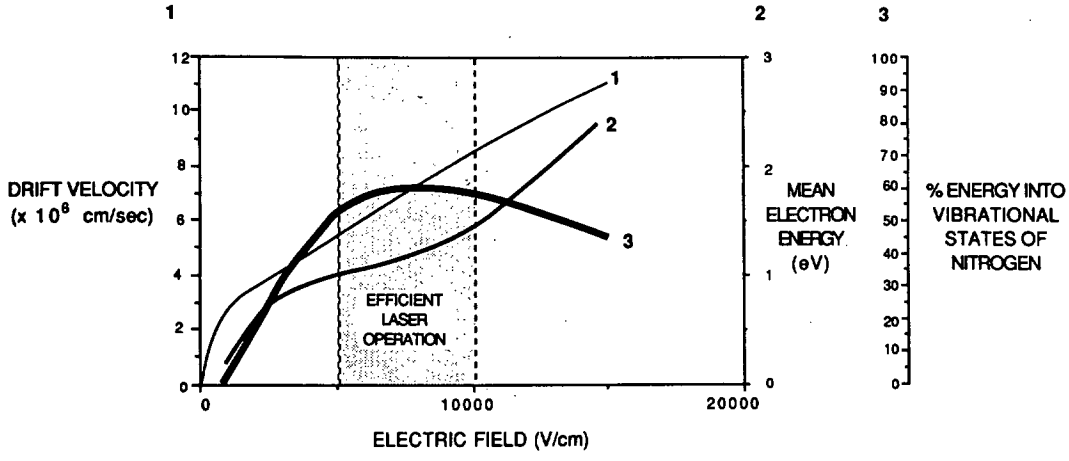

FIG. 4. Dependence of the electron temperature, drift velocity, and the vibrational excitation efficiency on the electric field in a 1-atm pressure, 3/2/1, $He/N_2/CO_2$ laser discharge.

C. Finite impedance case

In this intermediate case [see Eq. (12)]

$$V_0/R = ev_d n_e S + (LE/R) = \text{const.} \tag{28}$$

Therefore, instead of Eq. (20), one has

$$\delta E = -v_{d0} \frac{\delta n_e}{(v'_{d0} + L/eRSn_{e0})n_{e0}}. \tag{29}$$

This shows that Eqs. (23)–(26) also holds in the finite impedance case if, in these equations, one replaces

$$v'_{d0} \rightarrow v'_{\text{deff}} \equiv v'_{d0} + L/eRSn_{e0}. \tag{30}$$

As $R \rightarrow \infty$, $v'_{\text{deff}} \rightarrow v'_{d0}$ and the stiff current discharge is recovered (except for the fact that V_0 is finite) (case B). If, in contrast, $R \rightarrow 0$ then $v'_{\text{deff}} \rightarrow \infty$ and $B \rightarrow 0$, which is the unstable case, corresponding to the stiff voltage conditions.

IV. NUMERICAL EXAMPLE

In this section the discharge model developed so far will be applied to the specific case of a CO_2 laser discharge. Before this can be done, however, one has to know the relevant rate constants for the CO_2 mixture as a function of the electric field. A 1-atm total pressure, 3/2/1, $He/N_2/CO_2$ mixture will be chosen as an example. The rate constants for the ionization and excitation of the electronic states of N_2 in this mixture, the fraction of discharge energy that goes into vibrational excitation and the drift velocity as predicted by the Boltzmann code[6] are shown in Figs. 4 and 5. From Fig. 4, which is a plot of T_e, v_d and the efficiency of exciting the vibrational levels of N_2, it is clear that efficient CO_2 laser operation occurs between 5 and 10 kV/cm.

Figure 5 shows the variation of ν and γ [see Eqs. (5) and (6)] as functions of the electric field. Also shown in Fig. 5 is the curve for the ionization rate from the ground state (ν_a). The curve for γ shown in Fig. 5 is the total excitation rate constant for all the electronic levels. This was chosen since it is difficult to identify the relevant metastable or electronic state that will be subsequently ionized. It is probable that this state will be a high-lying state such as the C state of N_2. The ionization rate constant ν of the excited electronic state has the same shape as the electron impact ionization rate of N_2 ($a\Sigma_u$).[7] Its magnitude, however, was increased by 10^2, since this state is about 9 eV below the ionization level of N_2 as opposed to the C level which is less than 4 eV below the ionization level. From Fig. 5 it is clear that $\nu_a \ll \nu$ in the region of interest and so for any reasonable metastable density ($n_m > 10^{12}$ cm^{-3}) the metastable ionization will be dominant. Figure 6 shows the recombination coefficient as a function of the electric field. Measurements of the recombination coefficient for a 3/2/1 laser mixture has been made for electric field strengths between 2.5 and 5 kV/cm.[6] The

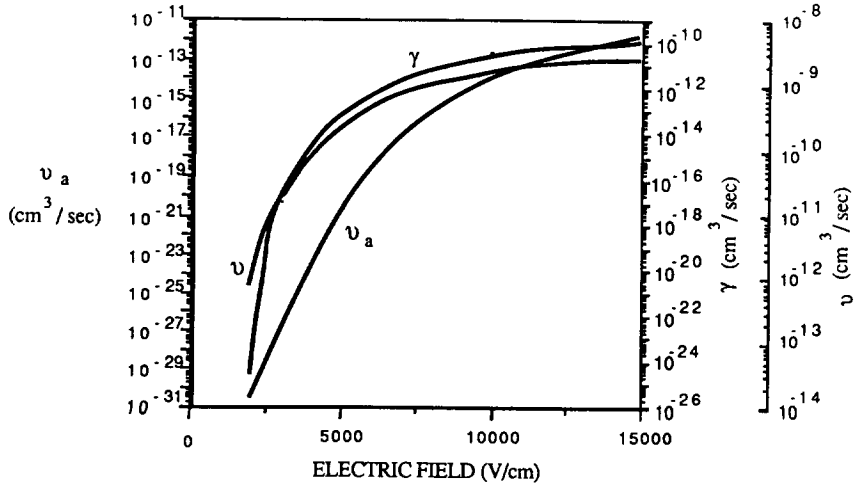

FIG. 5. Dependence of various excitation rates in a 1-atm, 3/2/1, CO_2 laser mixture discharge on the electric field. ν_a is the ionization rate from the ground state, ν is the indirect ionization rate, and γ is the total excitation rate from the ground state.

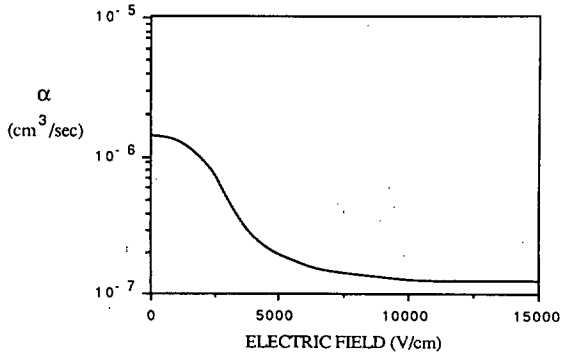

FIG. 6. Dependence of the recombination rate on the electric field in a 1-atm, 3/2/1, CO_2 laser mixture discharge.

curve shown in Fig. 6 makes use of these measurements and assumes an almost constant recombination rate for $10 < E < 15$ kV/cm.

At this stage the stability of the discharge at various operating conditions will be analyzed. The analysis will be started by presenting the dependence of functions $F(E)/S$ on the electric field [see Eq. (11)]. This dependence is shown in Fig. 7 for the case of interest. One observes that $E^* \simeq 8.05$ kV/cm, so that the steady-state discharge operation is possible for 8.05 kV/cm $< E <$ 15 kV/cm (see the discussion in Sec. II and Figs. 2 and 3). The graphical solution for the electric field E_0 in the steady-state discharge is also shown under the following conditions: $V_0 = 9$ kV, $RS = 400\,\Omega\,\text{cm}^2$, $L = 1$ cm, $\tau = 1\,\mu$s, and $\beta_0 = 10^5\,\text{s}^{-1}$. The steady-state electric field is 8.45 kV/cm which, by using Eq. (8), and data in Figs. 4–6, yields the steady-state plasma density $n_{e0} = 1.07 \times 10^{12}\,\text{cm}^{-3}$. Prior to studying the stability of the discharge at these conditions, the stiff voltage situation is considered. The analysis in Sec. III shows that the discharge in *unstable* in the stiff voltage case for $\beta_0 \neq 0$. This unstable behavior is demonstrated in Figs. 8 and 9, where the

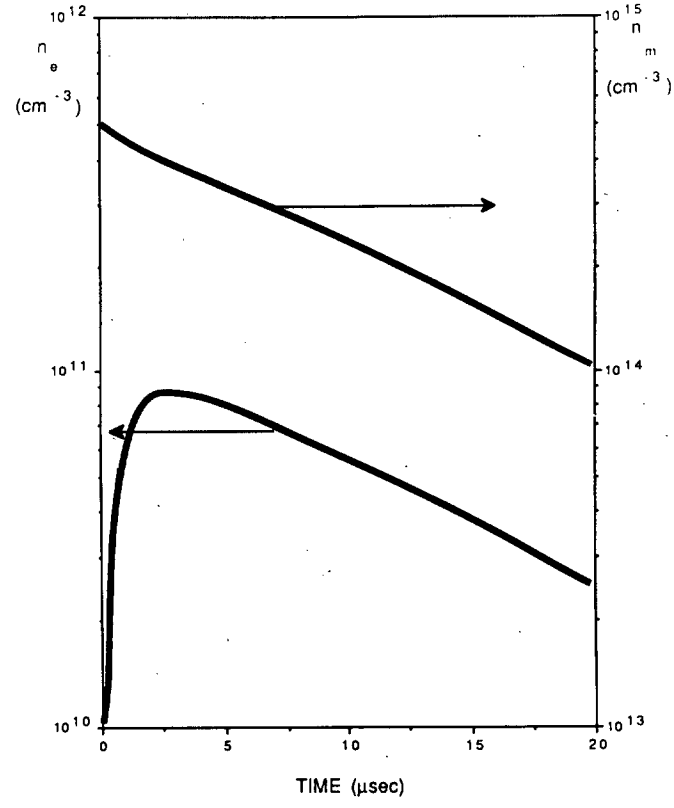

FIG. 8. Time evolution of the electron and metastable densities in a stiff voltage discharge. The initial electron density $[n_e(0) = 5 \times 10^{11}\,\text{cm}^{-3}]$ is lower than the steady-state density ($n_{e0} = 1.07 \times 10^{12}\,\text{cm}^{-3}$) at the given voltage ($V_0 = 8.45$ kV).

numerical solutions of Eqs. (5) and (6) are shown for $E_0 = 8.45$ kV/cm = const (stiff voltage condition) and two different initial values for the electron density. The electric field E_0 defines various rates in Eqs. (5) and (6) which remain constants in the calculations, consistent with the stiff voltage conditions. Figure 8 shows the case when $n_e(0)$

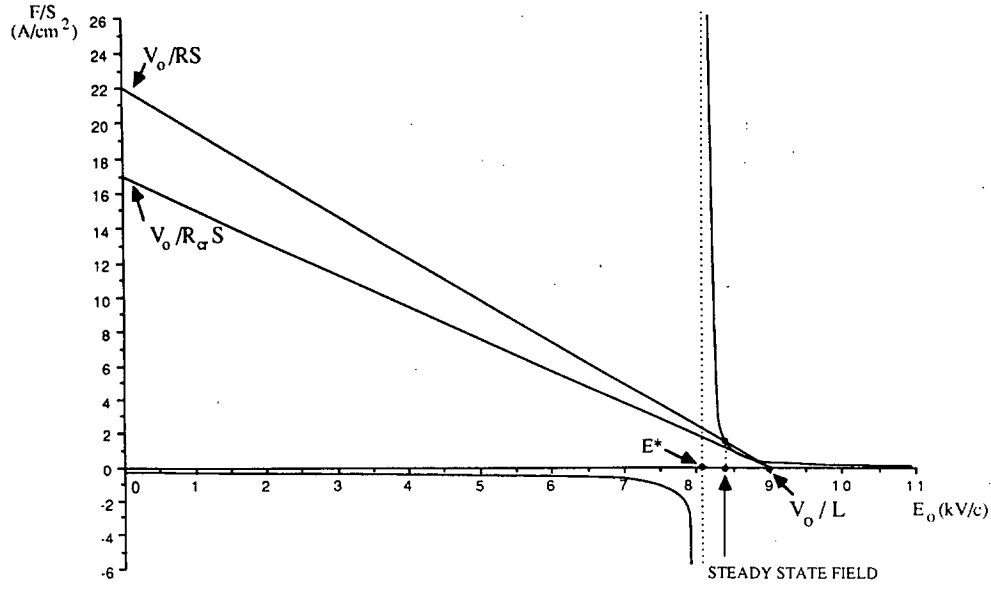

FIG. 7. Dependence of F/S on the electric field in a 1 atm, CO_2 laser discharge mixture. The operating field ($E_0 = 8.45$ kV/cm) is found graphically for the case: $V_0 = 9$ kV/cm, $RS = 400\,\Omega\,\text{cm}^2$, $L = 1$ cm, $\tau = 1\,\mu$s, and $\beta_0 = 10^5\,\text{s}^{-1}$. The straight line tangent to the curve F/S allows to determine the critical impedance ($R_{cr}S = 520\,\Omega\,\text{cm}^2$).

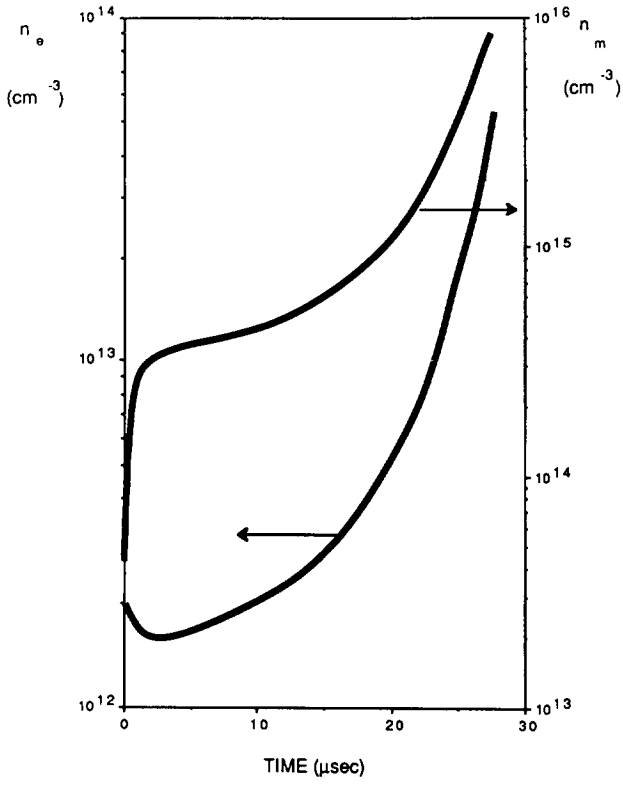

FIG. 9. Time evolution of the electron and metastable densities in a stiff voltage discharge with attachment. Initial electron density (2×10^{12} cm^{-3}) is higher than the steady-state density ($n_{e0} = 1.07\times10^{12}$ cm^{-3}) at the given voltage ($V_0 = 8.34$ kV).

$= n_m(0) = 5\times10^{11}$ cm^{-3}. This initial density is lower than the above-mentioned steady-state density ($n_{e0} = 1.07\times10^{12}$ cm^{-3}). Figure 8 shows that the electron density decays in time, in this case, and the discharge is quenched. Figure 9, in contrast, shows the case of $n_e(0) = 2\times10^{12}$ cm^{-3} which is larger than the steady-state electron density n_{e0}. n_e then grows indefinitely in time, verifying the instability. One finds that Figs. 8 and 9 represent the general time evolution of the discharge in the stiff voltage case, depending on whether $n_e(0)$ is larger or smaller than n_{e0}.

At this point it is appropriate to proceed to the numerical simulation of the finite external impedance discharge case. Again setting $V_0 = 9$ kV/cm, $L = 1$ cm, $\tau = 1\,\mu$s, and $\beta = 10^5\,\mathrm{s}^{-1} = \mathrm{const}(t)$. Nevertheless, in contrast to the stiff voltage case, the rate Eqs. (5) and (6) have now been solved simultaneously with the circuit Eq. (28). The code also makes use of the dependencies of the rate constants shown in Figs. 4–6. The predictions of the code are plotted in Figs. 10–12. Figure 10 shows the temporal variation of n_e and E for the circuit impedance of $RS = 400\ \Omega$ cm^2. The initial electron density was assumed to be 10^{12} cm^{-3}. One observes that the electron density increases by about 10% to 1.07×10^{12} cm^{-3} and the electric field decreases from its initial value of 9 kV/cm to 8.45 kV/cm. These are the steady-state electron density and the electric field under the above conditions (see the graphical solution in Fig. 7). Figure 11 shows the effect of lowering the external impedance to $RS = 1\Omega$ cm^2. Under these conditions, as can be seen in the figure, the discharge has stiff voltage characteristics during the first $\sim 10\,\mu$s of the

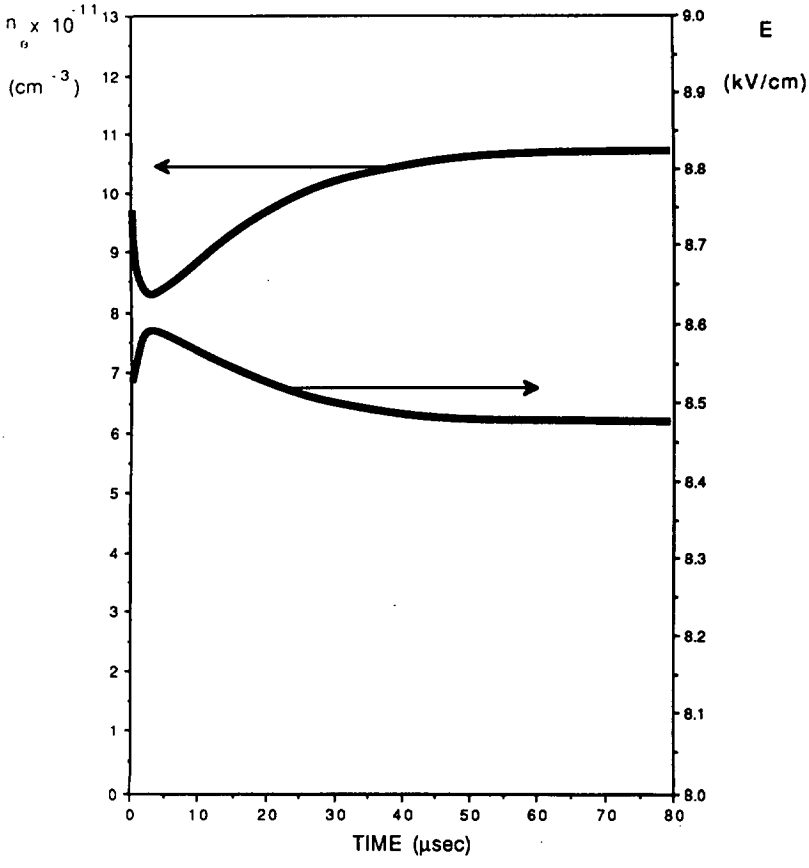

FIG. 10. Curves of n_e and E for a volumetrically stable discharge. The parameters are $n_e(0) = 10^{12}$ cm^{-3}, $V_0 = 9$ kV/cm, $RS = 400\,\Omega$ cm^2, $L = 1$ cm, $\tau = 1\,\mu$s and $\beta = 10^5\,\mathrm{s}^{-1}$.

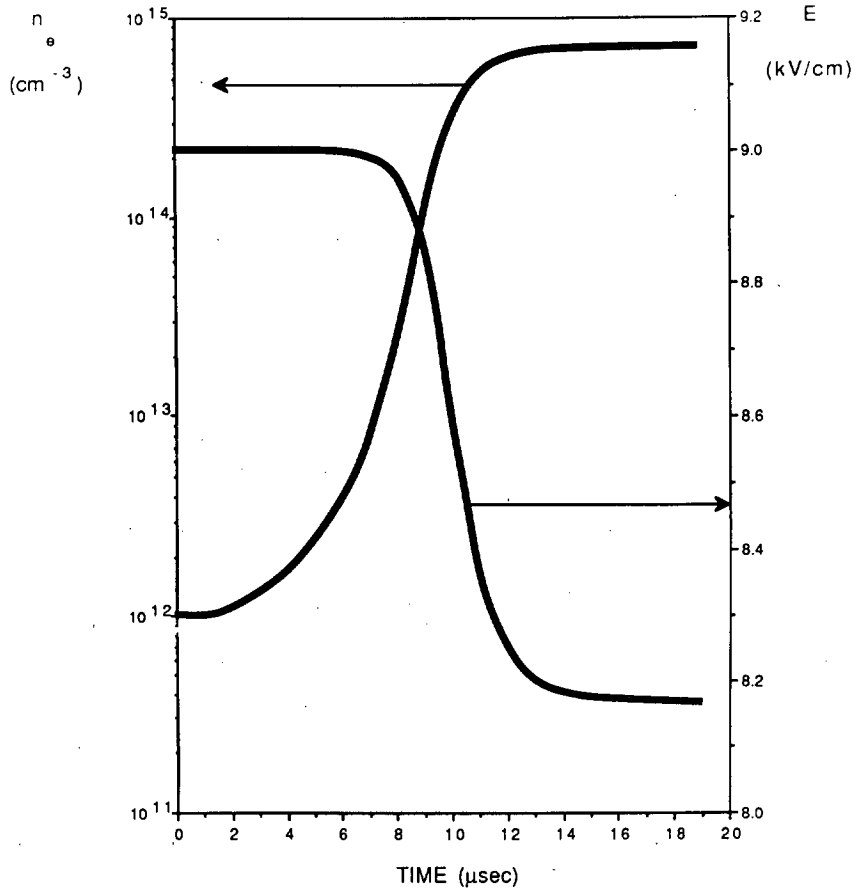

FIG. 11. Curves of n_e, and E for a low external impedance discharge ($RS = 1\ \Omega\ \text{cm}^2$). The parameters are $n_e(0) = 10^{12}\ \text{cm}^{-3}$, $V_0 = 9\ \text{kV/cm}$, $L = 1\ \text{cm}$, $\tau = 1\ \mu\text{s}$, and $B = 10^5\ \text{s}^{-1}$. The discharge is unstable during the initial evolution phase ($t < 15\ \mu\text{s}$).

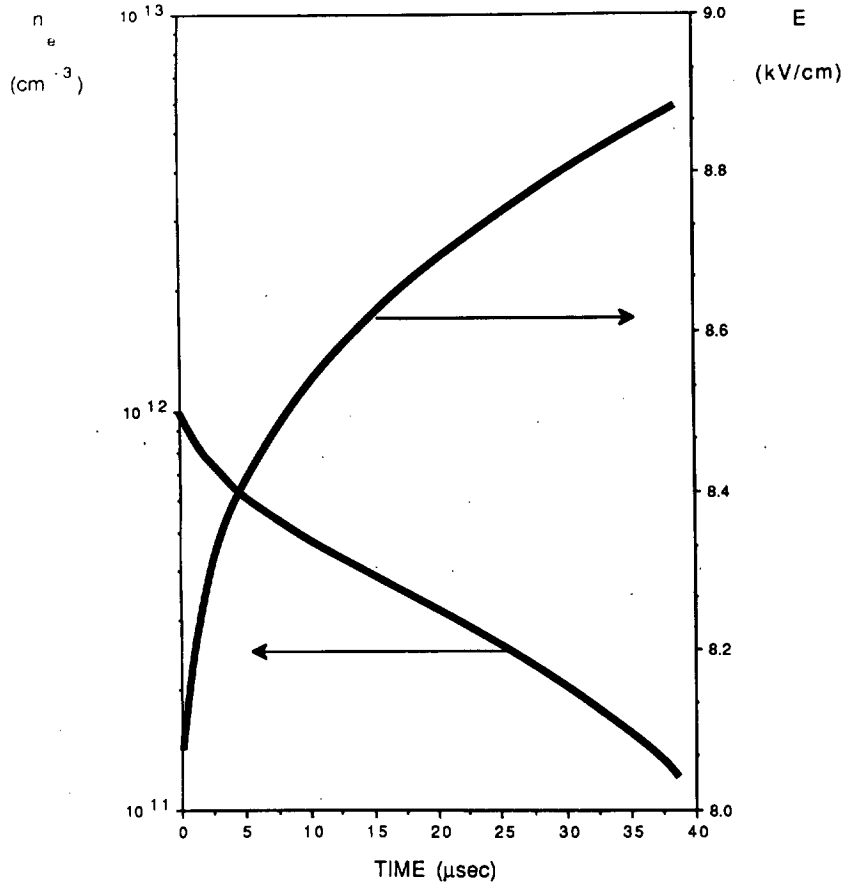

FIG. 12. Curves of n_e and E for a discharge with an above-critical impedance ($RS = 800\ \Omega\ \text{cm}^2$). All other parameters are the same as in Figs. 10 and 11. No steady state exists for $RS > R_{cr}S = 520\ \Omega\ \text{cm}^2$ and the discharge is quenched.

discharge. It is unstable as predicted by the analysis and the electron density suddenly increases by almost three orders of magnitude after 10 μs. The discharge becomes stable at this large value of $n_e \sim 8\times 10^{14}$ cm^{-3}. However, in practice, any initial spatial nonuniformities in n_e amplified in time by the instability could result in streamer formation during the fast transition period. We shall consider the details of such *spatial* instabilities in our future studies. Finally, Fig. 12 illustrates a typically situation in a discharge with an above-critical external impedance ($R > R_{cr}$, see the discussion in the previous section). In the case considered (see Fig. 7) $R_{cr} \simeq 520\ \Omega\ \text{cm}^2$, while the results presented in Fig. 12 correspond to the case $R = 800\ \Omega\ \text{cm}^2$. No steady state exists in this case, as predicted by the theory, and one observes in Fig. 12 that the discharge is quenched.

V. CONCLUSIONS

(i) We have considered the volumetric stability dynamics of discharges dominated by *two-step ionization*. In the presence of an attacher these discharges are shown to be potentially unstable on much shorter time scales than those characteristic of conventional thermal instabilities.

(ii) The theoretical modeling of the discharge included the discharge kinetics coupled to the *external electric circuit* and its response to varying current conditions. A number of discharge configurations, such as stiff voltage, stiff current, and finite external impedance were considered in searching for a steady-state stable regime of operation.

(iii) In the stiff voltage discharge (the electric field in the discharge $E = \text{const}$) the steady state exists for $E > E^*$, where E^* is the value at which the characteristic function $Q(E)$ [see Eq. (9)] vanishes. Nevertheless, even if the steady state is reached, the discharge is volumetrically unstable under the stiff voltage condition. Practically, if at $t = 0$ the initial electron density $n_e(0) > n_{e0}$ (n_{e0} being the steady-state density) the current density j increases indefinitely on a finite time scale, while for $n_e(0) < n_{e0}$ the discharge is quenched [$j(+) \to 0$]. The linear instability temporal rate is typically proportional to the attachment rate β (if β is sufficiently small).

(iv) The stiff current discharge ($j = \text{const}$) has a steady state at *all* currents and the discharge is volumetrically stable, provided the characteristic function $F(E)$ [see Eq. (11)] is *decreasing* function of the electric field.

(v) In the finite external impedance discharge case we found the existence of a critical impedance value R_{cr} such that there exist two steady states when $0 < R < R_{cr}$ and no steady state is possible when $R > R_{cr}$. Furthermore, only if R_{cr} is large enough, the above-mentioned steady-state solutions are stable in a part of the interval $[0, R_{cr}]$.

(vi) The theoretical predictions were illustrated in the example of an atmospheric CO_2 laser discharge model. The numerical solutions of the kinetic and external circuit equations underlying the problem in this case were found in an agreement with the theory.

ACKNOWLEDGMENT

This work was supported by the U.S. Army Missile Command, Contract No. DAAH01-86-C-1074.

[1] W. L. Nighan and W. J. Wiegand, Appl. Phys. Lett. **25**, 633 (1974).
[2] E. F. Jaeger and A. V. Phelps, Bull. Am. Phys. Soc. **19**, 147 (1974).
[3] S. M. Meerkov and G. I. Shapiro, Avtomat. Telemekhan. (in Russian) **6**, 12 (1976).
[4] J. D. Daugherty, J. A. Mangano, and J. H. Jacob, Appl. Phys. Lett. **28**, 581 (1976).
[5] D. H. Douglas-Hamilton (private communication).
[6] D. H. Douglas-Hamilton and R. S. Lowder, "Avco Everett Research Laboratory Kinetics Handbook" (1974) (unpublished).
[7] C. E. Caldonia, S. J. Davis, B. D. Green, L. G. Piper, W. T. Rawlins, G. A. Simons, and G. M. Weyl, "Analysis of Metastable State Production and Energy Transfer," Report No. AFWAL-TR-86-2078 (1986).